

## MATHEMATICAL MODEL OF THE CURRENT TIME FOR THREE-FRAGMENT RADAR SIGNAL WITH NON-LINEAR FREQUENCY MODULATION

**Kostyria O. O.** – Dr. Sc., Senior Research, Leading Research Scientist, Ivan Kozhedub Kharkiv National Air Force University, Kharkiv, Ukraine.

**Hryzo A. A.** – PhD, Associate Professor, Head of the Research Laboratory, Ivan Kozhedub Kharkiv National Air Force University, Kharkiv, Ukraine.

**Dodukh O. M.** – PhD, Leading Research Scientist, Ivan Kozhedub Kharkiv National Air Force University, Kharkiv, Ukraine.

**Nareznyi O. P.** – PhD, Associate Professor, V. N. Karazin Kharkiv National University, Kharkiv, Ukraine.

**Fedorov A. V.** – PhD, Research, Ivan Kozhedub Kharkiv National Air Force University, Kharkiv, Ukraine.

### ABSTRACT

**Context.** The authors of the article have developed a new mathematical model that allows taking into account frequency and phase distortions that occur in a three-fragment signal during the transition from one fragment to another, when the rate of frequency modulation of the signal changes. The object of research is the process of formation and processing of radar non-linear frequency modulation signals.

**Objective.** The purpose of the work is to develop and research a mathematical model of current time for a signal with non-linear frequency modulation, which consists of three linear frequency modulated fragments.

**Method.** The article provides a theoretical justification of the need to develop a mathematical model in the current time for a three-fragment signal with non-linear frequency modulation, capacity for work of the created model is demonstrated on the example of several radio signals that differ in frequency parameters. With the same signal parameters, the obtained results were compared with the results of the known model, for which known methods of spectral and correlation analysis were used. A distinctive feature of the proposed model is the consideration of jumps in the instantaneous frequency and phase of the signal that occur during the transition from one linear-frequency modulated fragment to the next. Such jump-like changes in frequency and phase in known models of signals with non-linear frequency modulation are not compensated for, which causes distortion of their spectra and an increase in the side lobes level of auto-correlation (mutual-correlation) functions.

**Results.** A comparative check of the developed and known signal models indicates a decrease in the side lobes level of the autocorrelation function by 3 dB or more, depending on the given frequency-time parameters.

**Conclusions.** The application of the proposed mathematical model makes it possible to form and process radar signals, which include three linear-frequency modulated fragments. Compensation of jump-like changes in frequency and phase leads to a decrease in the degree of distortion of the spectrum and, as a result, an increase in its effective width, which ensures a narrowing of the main lobe and a decrease in the side lobes level of the auto-correlation function.

**KEYWORDS:** radar signal; non-linear frequency modulation; autocorrelation function, side lobe level; mathematical model.

### ABBREVIATIONS

ACF is an autocorrelation function;  
LFM is a linear frequency modulation;  
ML is a main lobe;  
MM is a mathematical model;  
NLFM is a non-linear frequency modulation;  
PSD is a power spectral density;  
PSLL is a peak side lobe level;  
RM is a radar mean;  
RFM is a rate of frequency modulation;  
RRD is a receiving device;  
WP is a weight processing.

### NOMENCLATURE

$\Delta f_n$  is a frequency deviation of the  $n^{\text{th}}$  signal fragment, Hz;  
 $f_{en}$  is a final frequency of the  $n^{\text{th}}$  signal fragment, Hz;  
 $\dot{U}(t)$  is a complex signal amplitude, V;  
 $f(t)$  is an instantaneous signal frequency, Hz;  
 $f_n(t)$  is a neural network model structure;

$\varphi(t)$  is an instantaneous signal phase, rad;  
 $\varphi_n(t)$  is an instantaneous phase of the  $n^{\text{th}}$  LFM signal fragment, rad;  
 $|\dot{U}(t)|$  is a complex signal amplitude module, V;  
 $n$  is a sequence number of the signal fragment ( $n=1, 2, 3$ );  
 $t$  is a current time, s;  
 $f_0$  is an initial signal frequency, Hz;  
 $f_{0n}$  is an initial frequency of the  $n^{\text{th}}$  signal fragment, Hz;  
 $\delta f_{mn}$  is a frequency jump when moving from the  $m = n - 1^{\text{th}}$  signal fragment to the  $n^{\text{th}}$ , Hz;  
 $\delta \varphi_{mn}$  is a phase jump at the transition from the  $m^{\text{th}}$  signal fragment to the  $n^{\text{th}}$ , rad;  
 $\Delta f_{12}$  is a total deviation of the frequency of the first and second signal fragments, Hz;  
 $T_s$  is a total duration of the NLFM signal, s;

$T_{12}$  is a total duration of the first and second signal fragments, s;

$T_n$  is a duration of the  $n^{\text{th}}$  signal fragment, s;

$\omega(t)$  is a cyclic frequency of the signal, rad/;

$\beta_n$  RFM of the  $n^{\text{th}}$  LFM signal fragment, Hz/s.

## INTRODUCTION

The widespread use of solid-state (transistor) transmission devices causes certain limitations regarding the peak power of probing signals, the designers are forced to use signals of increased duration, which leads to a deterioration of the range resolution.

In order to overcome the contradiction between the need to increase the duration of probing radio pulses and maintain the necessary resolution of RM, signals with intra-pulse frequency (phase) modulation (manipulation) have become widely used [1–6].

Historically, LFM signals were the first to be used due to the ease of implementation of devices for their formation and processing. However, a significant disadvantage of such signals is the relatively high PSLL of their ACF, which is approximately  $-13$  dB [1, 2], which in some situations requires raising the detection threshold in systems for stabilizing the level of false alarms and, in general, worsens the potentially achievable detection characteristics signals reflected from targets.

One of the most common methods of reducing PSLL is the application of WP in the time or frequency domain (time or spectral windows) [7–9]. It is possible to achieve an even greater reduction of PSLL by using NLFM of the probing signal followed by traditional WP in RRD [2, 10, 11]. In [2, 12, 13], it is proposed to use a signal consisting of three NLFM fragments adjacent to each other in time with a successive increase or decrease in the instantaneous frequency as such an LFM signal. The peculiarity of this signal is that the extreme fragments have a smaller value of the PSD due to the fact that they have a larger RFM  $\beta_n$ , which is determined by the ratio of the deviation of the frequency of the  $n$ -th LFM fragment  $\Delta f_n$  to its duration  $T_n$ ,  $\beta_n = \Delta f_n / T_n$ . Such a decrease in the PSD at lower and upper frequencies leads to a rounding of the resulting spectrum, as a result of which there is a decrease the PSLL [2, 13] with the expansion the ML of the ACF due to a decrease in its effective width. The expansion the ML leads to a decrease in the resolution of the RM from a distance, which is not always acceptable.

The traditional approach is to choose a compromise solution, that is, to achieve the required PSLL value with a slight permissible deterioration of the specified resolution.

The approach based on the use of different types of signals in accordance with the tasks of the RM has potentially greater advantages.

This work is devoted to the development of a mathematical model of a three-fragment NLFM signal with concoct of three LFM fragments, with the possibility of

further implementation of such signals in existing RM and those under development.

**The object of study** is the process of formation and processing of radar NLFM signals.

**The subject of study** is mathematical models of NLFM signals.

**The purpose of the work** is to theoretically substantiate the need to develop and design a MM of an NLFM signal consisting of three LFM fragments, as well as to test its workability.

## 1 PROBLEM STATEMENT

Among the MMs of three-fragment NLFM signals, the most commonly used are the MMs in which the input values are the current time  $t$ , the duration of the fragments  $T_n$ , and the deviation of their frequency  $\Delta f_n$ , which is equal to the difference between the final and initial frequencies of the corresponding  $n$ -th LFM fragment and is a fixed value. It is determined by the product of the RFM of the  $n$ -th LFM signal fragment  $\beta_n$  and its duration  $T_n$ .

$$\Delta f_n = f_{en} - f_{0n} = \beta_n T_n.$$

In general, the complex signal amplitude is represented as:

$$\dot{U}(t) = |\dot{U}(t)| \exp\{j\varphi(t)\}. \quad (1)$$

To simplify the following, we assume  $|\dot{U}(t)| = 1$ .

The functions of changing the instantaneous frequency and phase of the signal for each  $n$ -th fragment are different, the change occurs during the transition from one fragment to the next.

The instantaneous frequency is proportional to the speed of the frequency-modulated  $n$ -th fragment and is linearly dependent on time:

$$f_n(t) = \beta_n t,$$

and the instantaneous phase, in turn, has linear and quadratic components and is determined by the dependence:

$$\varphi_n(t) = 2\pi \left( f_{0n} t + \frac{\beta_n t^2}{2} \right).$$

The total duration of the NLFM signal is defined as the sum of the durations of the LFM fragments:

$$T_s = \sum_{n=1}^3 T_n,$$

$T_{12} = T_1 + T_2$  – total duration of the first and second signal fragments.

Well-known relations interconnect the instantaneous frequency and phase [1–2]:

$$\varphi(t) = \int f(t)dt ;$$

$$f(t) = \frac{d\varphi(t)}{dt} .$$

To make the formulas more compact, we introduce the notation of the total frequency deviation of the first and second signal fragments:

$$\Delta f_{12} = \Delta f_1 + \Delta f_2 .$$

Further analysis will be carried out by graphically comparing the realizations of signals in the time and frequency domains, their ACF, and the dependence of the instantaneous frequency and phase of signals on time. The signals will be compared by the level of their PSLL at a fixed WP width, or by comparing the degree of WP expansion at a constant level of PSLL.

## 2 REVIEW OF THE LITERATURE

Many publications have been devoted to the formation and processing of NLFM signals in various fields of application, with the most extensive studies of such signals in the field of air target radar [14–18]. In works [15–16], the potentially achievable PSLL of the ACF is estimated for a three-frame-segment NLFM signal, the range resolution of the RM is analyzed in detail [17], and the effect of the Doppler frequency shift on the characteristics of the ACF is studied [17–18].

Another area related to the use of NLFM signals is meteorological localization, with the peculiarity that the main research direction in this area is to study the problem of reducing the PSLL [19]. A similar problem with respect to RM with a synthesized antenna aperture is discussed in detail in [20–23].

A distinctive feature of papers [14, 24–25] is that to minimize the PSLL, it is proposed to use only NLFM signals, or to combine their use with additional WP in the RDD [2, 17, 19].

Papers [11, 19, 26–27] use mathematical models of NLFM signals of the current time with a smooth (polynomial) change in the frequency modulation law.

The formation of NLFM signals from three LFM fragments was proposed in [2, 12, 13], where the MM is presented, in which the argument (time) changes symmetrically in the middle of the radio pulse. Subsequently, to represent such signals, a mathematical technique is used in which each subsequent fragment starts from a zero time reference (from the zero phase), that is, each time the time is shifted to the zero mark [16, 18, 24, 25, 28–30].

Research has shown that the introduced MM do not fully reflect the peculiarities of the formation of NLFM signals, namely, they do not take into account the phase structure of the signal at the junctions of fragments.

In authors propose to consider the MM of a three-fragment NLFM signal developed by the authors, which is a further development of the MM presented in [2, 12, 13, 31]. Unlike the existing ones, the model more adequately takes into account the phase change at the junctions of LFM signal fragments, preventing the appearance of instantaneous frequency and phase jumps, which allows us to obtain a lower PSLL.

## 3 MATERIALS AND METHODS

Further analysis is performed using a common MM of a three-fragment NLFM signal introduced in [16, 18, 24, 25, 28–30]. The peculiarity of this MM is that the determination of the instantaneous amplitude (1) for all LFM fragments starts from zero time by shifting the time scale by the duration of the previous signal components. For example, for an NLFM signal consisting of three LFM fragments, the complex signal amplitude is described in accordance with (2).

$$\dot{U}(t) = |\dot{U}(t)| \begin{cases} \exp(j\varphi_1(t)), & 0 \leq t \leq T_1; \\ \exp(j\varphi_2(t - T_1)), & T_1 \leq t \leq T_{12}; \\ \exp(j\varphi_3(t - T_{12})), & T_{12} \leq t \leq T_3. \end{cases} \quad (2)$$

In the future, to record the expressions of the phase and frequency of the NLFM signal fragments, we assume that time intervals similar to (2) are applied to them.

The instantaneous phases of the signal (2) can be found by expressions [16, 18, 24–25, 28–30]:

$$\varphi(t) = 2\pi \begin{cases} f_0 t + \frac{\beta_1 t^2}{2}; \\ (f_0 + \Delta f_1)(t - T_1) + \frac{\beta_2 (t^2 - T_1 t)}{2}; \\ (f_0 + \Delta f_{12})(t - T_{12}) + \frac{\beta_3 (t^2 - T_{12} t)}{2}. \end{cases} \quad (3)$$

By differentiating the expressions of the instantaneous phase (3), the ratios for the instantaneous frequency of the corresponding signal fragments are found [16, 18, 24–25, 28–30]:

$$f(t) = \begin{cases} f_0 + \beta_1 t; \\ f_0 + \Delta f_1 + \beta_2 (t - T_1); \\ f_0 + \Delta f_{12} + \beta_3 (t - T_{12}). \end{cases} \quad (4)$$

A significant drawback of MM (3) – (4) is that due to the shift of the time scale to zero for each subsequent fragment, this model is not sensitive to abrupt changes in instantaneous frequency that occur at the moments of increase or decrease in the RFM (at the junctions of fragments).

The graph of the signal frequency versus time for (4) is shown in Fig. 1.

From the analysis of Fig. 1 and (4), it follows that the initial frequency of the second LFM fragment has the value of  $f_0 + \Delta f_1$ , when in fact it is equal to  $f_{02}$ . Accordingly, the initial phase of the second fragment has a zero value, while the final phase of the first fragment is equal to  $\varphi_{e1} = 2\pi(f_0 + \Delta f_1)T_1$ . That is, at the moment  $t = T_1$  there is an abrupt change in the instantaneous frequency and instantaneous phase of the signal.

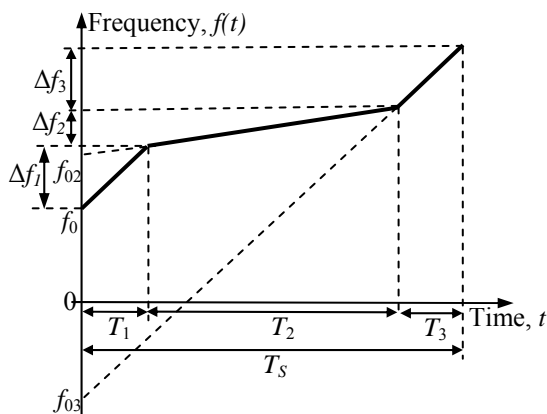


Figure 1 – Graph of changes in the frequency of the NLFM signal consisting of three LFM fragments

The same situation is observed at the junction of the second and third fragments at  $t = T_1 + T_2$ , the initial frequency of the third fragment is equal to :

$$f_{03} = f_0 + \Delta f_1 + \Delta f_2,$$

and its actual value is  $f_{03}$  with a “minus” sign.

For further consideration, we obtain analytical expressions that determine the values of frequency and phase jumps for the time instant  $t = T_1$ .

The final value of the frequency of the LFM signal of the first fragment at time  $t = T_1 - \delta t$ , under the condition  $\delta t \rightarrow 0$  is described by the expression

$$f_{e1} = f_0 + \beta_1 T_1,$$

and the initial frequency value for the second signal fragment at time  $t = T_1 + \delta t$  is

$$f_{02} = f_0 + \beta_2 T_1.$$

Thus, the frequency jump at this point in time is equal to their difference:

$$\delta f_{12} = f_{02} - f_{e1} = (\beta_2 - \beta_1)T_1. \quad (5)$$

By integrating, we find the corresponding signal phase jump:

$$\delta \varphi_{12} = \int_0^{T_1} (\beta_2 - \beta_1)T_1 dt = \frac{1}{2}(\beta_2 - \beta_1)T_1^2. \quad (6)$$

The next jump in the frequency-phase parameters of the signal occurs when we move to the third LFM fragment. Let's extend the line segment (Fig. 1), which demonstrates the change in the frequency of this fragment, to the intersection with the abscissa axis and mark the intersection point as  $f_{03}$ , i.e., this is the conditional initial frequency of the third fragment. From the analysis of Fig. 1, it turns out that the frequency jump at the moment of transition from the second signal fragment to the third  $\delta f_{23}$ , similar to (5), is:

$$\delta f_{23} = f_0 + \beta_1 T_1 + \beta_2 T_2 - \beta_3 T_{12}.$$

After simplification, we get:

$$\delta f_{23} = (\beta_3 - \beta_1)T_1 + (\beta_3 - \beta_2)T_2. \quad (7)$$

By integrating over the appropriate time intervals, similar to (6), we find the expression for the phase jump:

$$\delta \varphi_{23} = \frac{1}{2}(\beta_3 - \beta_1)T_1^2 + \frac{1}{2}(\beta_3 - \beta_2)T_2^2. \quad (8)$$

Thus, based on (5)–(8), it can be concluded that the process of forming a NLFM signal consisting of three LFM fragments is accompanied by a jump-like change in the instantaneous frequency at the moment of transition from one fragment to the next, which causes a corresponding jump in the instantaneous phase of the signal. In the MM with a time shift (3)–(4), these jumps are not taken into account, which is its essential drawback. For further use, it is proposed to introduce a new MM of the NLFM of a signal in the current time, which takes into account the jumps in instantaneous frequency and phase.

To record the values of the instantaneous phase of a three-fragment NLFM signal in the current time, we use the well-known model of three LFM fragments [16]. The formula uses the same time intervals as in (2):

$$\varphi(t) = 2\pi \begin{cases} f_0 t + \frac{\beta_1 t^2}{2}; \\ (f_0 + \beta_1 T_1)t + \frac{\beta_2 t^2}{2}; \\ (f_0 + \beta_1 T_1 + \beta_2 T_2)t + \frac{\beta_3 t^2}{2}. \end{cases} \quad (9)$$

By differentiating the expressions (9) for the instantaneous frequency, we have the following:

$$f(t) = \begin{cases} f_0 + \beta_1 t; \\ f_0 + \beta_1 T_1 + \beta_2 t; \\ f_0 + \beta_1 T_1 + \beta_2 T_2 + \beta_3 t. \end{cases} \quad (10)$$

For further consideration, firstly, we obtain an intermediate MM by compensating for the frequency jump taking into account (5) and (7), MM (9) takes the form:

$$\varphi(t) = 2\pi \begin{cases} f_0 t + \frac{\beta_1 t^2}{2}; \\ [f_0 - (\beta_2 - \beta_1)T_1]t + \frac{\beta_2 t^2}{2}; \\ [f_0 - (\beta_3 - \beta_1)T_1 - (\beta_3 - \beta_2)T_2]t + \frac{\beta_3 t^2}{2}, \end{cases} \quad (11)$$

and the signal frequency changes as:

$$f(t) = \begin{cases} f_0 + \beta_1 t; \\ f_0 - (\beta_2 - \beta_1)T_1 + \beta_2 t; \\ f_0 - (\beta_3 - \beta_1)T_1 - (\beta_3 - \beta_2)T_2 + \beta_3 t. \end{cases} \quad (12)$$

To compensate for phase jumps (6) and (8), we add the corresponding components to (10) and obtain the final MM of the current time for the three-fragment NLFM of the signal:

$$\varphi(t) = 2\pi \begin{cases} f_0 t + \frac{\beta_1 t^2}{2}; \\ [f_0 - (\beta_2 - \beta_1)T_1]t + \frac{\beta_2 t^2}{2} + \delta\varphi_{12}; \\ [f_0 - (\beta_3 - \beta_1)T_1 - (\beta_3 - \beta_2)T_2]t + \frac{\beta_3 t^2}{2} - \delta\varphi_{23}, \end{cases} \quad (13)$$

whose frequency changes in accordance with (12).

It should be noted that the transition from the first LFM of a fragment to the second is accompanied by a decrease in the RFM, so the additional phase shift has a positive value, and during the next transition the RFM increases, and therefore the phase shift is negative.

To verify the adequacy and reliability of the developed model, simulation modeling was carried out in the MatLab application package.

#### 4 EXPERIMENTS

The MM of the three-fragment NLFM signal was verified for the following LFM parameters of the fragments:  $f_0 = 0$ ,  $\Delta f_1 = \Delta f_3 = 165$  kHz,  $\Delta f_2 = 400$  kHz,  $T_1 = T_3 = 20$   $\mu$ s,  $T_2 = 100$   $\mu$ s.

The simulation was performed sequentially in accordance with (3) – (4), (9) – (10), (11) – (12), and (13). The

simulation results are displayed in the form of graphs of frequency changes and time realizations in the current time, their spectra, and ACF.

#### 5 RESULTS

The results of mathematical modeling using (3)–(4) are shown in Fig. 2. The graph of changes in the frequency of the NLFM signal (Fig. 2a) and its oscilloscope frame  $U(t) = |\dot{U}(t)|$  (Fig. 2b) are plotted in the same time interval.

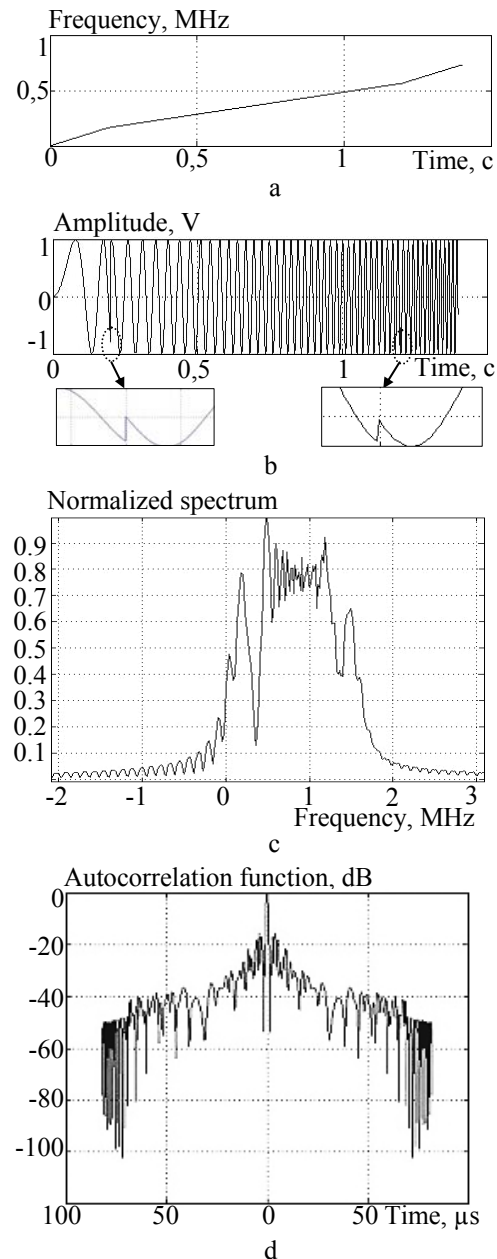


Figure 2 – Graph of instantaneous frequency change (a), oscilloscope (b), spectrum (c), ACF (d) of the NLFM signal with parameters  $\Delta f_1 = \Delta f_3 = 165$  kHz,  $\Delta f_2 = 400$  kHz,

$$T_1 = T_3 = 20 \mu\text{s}, T_2 = 100 \mu\text{s}$$

The analysis of the graphs shows that abrupt changes in the instantaneous phase of the signal (Fig. 2b, the enlarged scale of the phase jumps is shown in the footnotes) occur at the moment of transition to the next LFM fragment (Fig. 2a). The spectrum of the NLFM signal  $S(f)$  (Fig. 2c) has dips at the transition frequencies (Fig. 2c), which indicates the presence of phase jumps at these frequencies, as evidenced by the pulsations on the spectrum slopes. The ACF signal  $R(\tau)$  is shown in Figure 2d. The PSLL of the ACF is  $-15.59$  dB, the width ML of the ACF is  $1.9 \mu\text{s}$ . There is a sharp change in the PSLL ACF in the time intervals corresponding to the signal region with a higher RFM value, which is also a sign of the presence of phase distortion.

In the course of modeling according to (9)–(10), the results of which are shown in Fig. 3, it was found that the signal frequency change graph in Fig. 3a, in contrast to Fig. 2a demonstrates the presence of instantaneous frequency jumps at the moments of change RFM (Fig. 3a); these moments correspond to jumps in the signal phase (Fig. 3b) with a clear increase in the frequency of oscillations at the beginning of each new fragment.

Due to the frequency jumps between signal fragments, its spectrum (Fig. 3c) has three separate components and clearly expressed pulsations of the steeples. A sharp drop in the PSLL ACF (Fig. 3d) with a sharp change in the frequency and level of the lateral lobe pulsations addi-

tionally indicates the presence of significant frequency and phase jumps in the signal.

The ACF parameters for this MM were not evaluated because of the obvious discrepancy between the obtained results and the expected ones. The obtained results prove the validity of (5)–(8) and the need to compensate for frequency and phase jumps during the transition to each new section of the NLFM signal.

The results of the next experiment allow us to compare the work of (3)–(4) and (11)–(12), since (4) and (12) demonstrate a complete coincidence of results, the graph of (12) is not shown.

The results of the modeling according to (11) are shown in Fig. 4. Despite the coincidence of the simulation results according to (4) and (12), the waveform in Fig. 4b shows a different character of the signal phase distortion during changes in the RFM with compared to Fig. 2b. The difference in phase jumps is evident in the spectra of Figs. 2c and Fig. 4c, the PSLL ACF in Fig. 4d is  $-17.31$  dB, and the width of the ML of the ACF is  $1.8 \mu\text{s}$ . Given that (3)–(4) are not sensitive to frequency jumps, and (11)–(12) compensate for frequency jumps, these models demonstrate differences in other signal features.

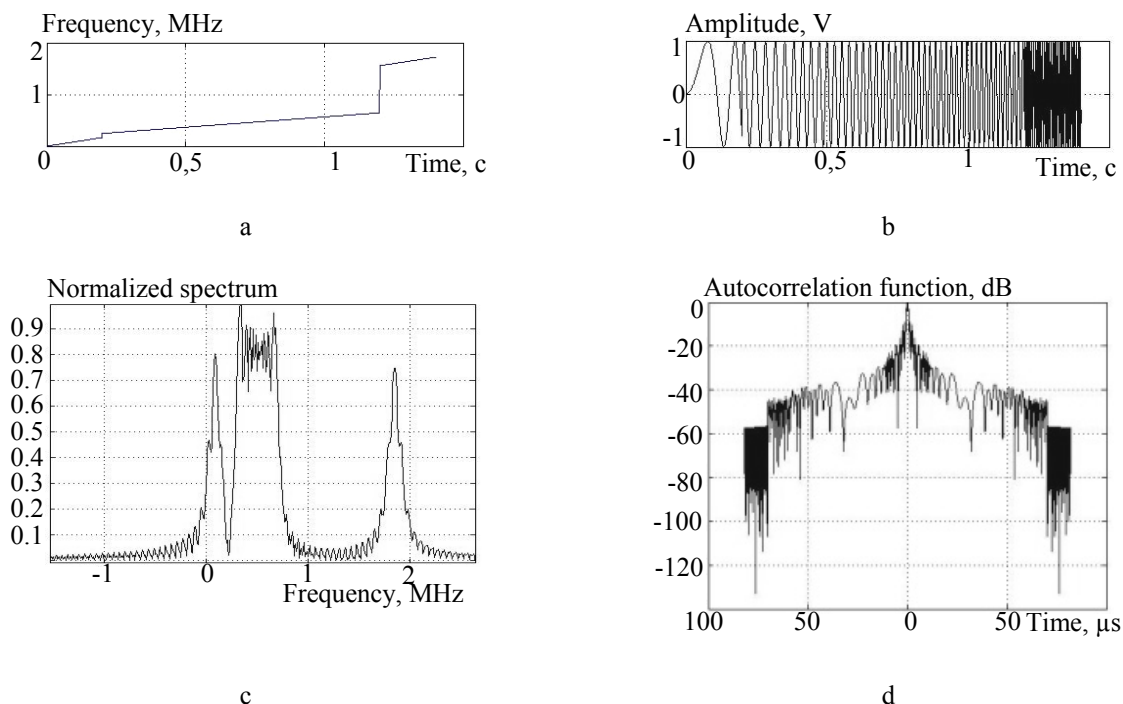


Figure 3 – Graph of instantaneous frequency change (a), oscilloscope (b), spectrum (c), ACF (d) of the NLFM signal without compensation for frequency and phase jumps

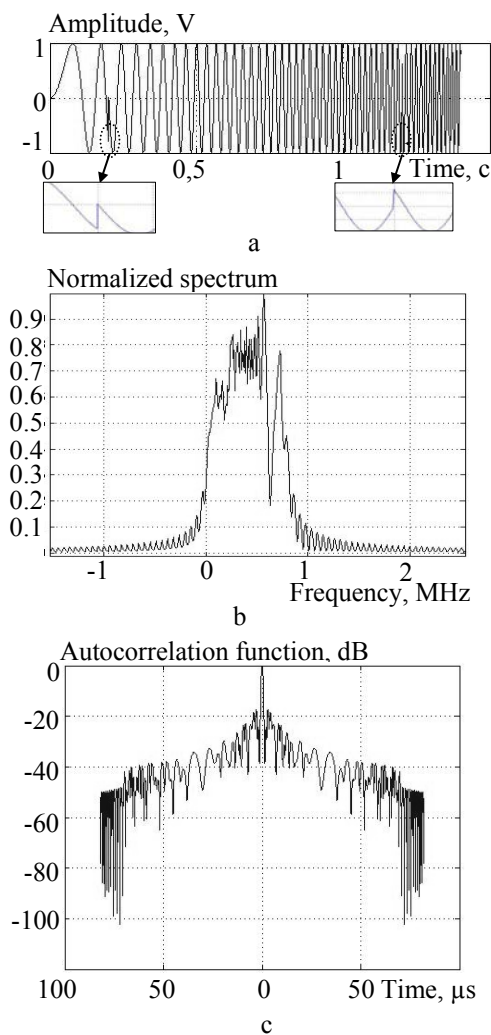


Figure 4 – Waveform (a), spectrum (b), ACF (c) of the NLFM signal with frequency jump compensation

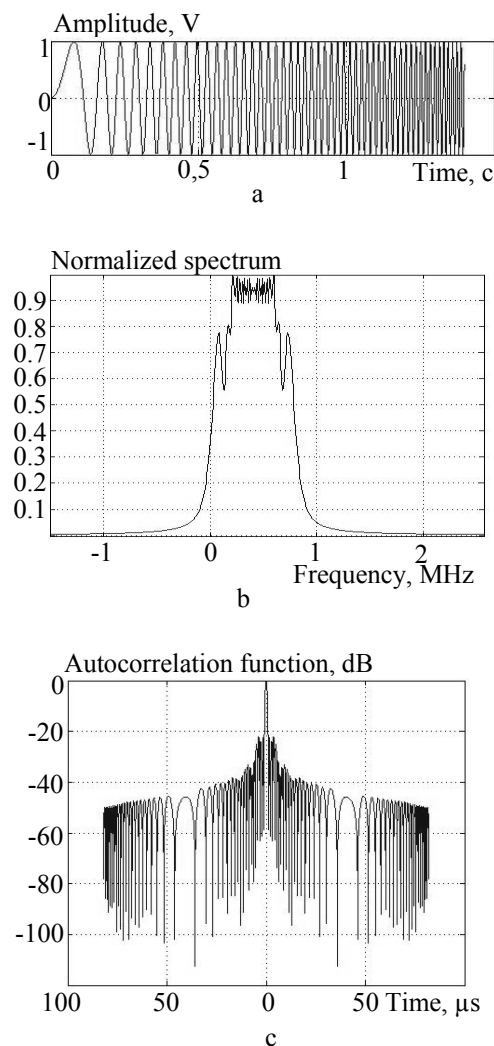


Figure 5 – Waveform (a), spectrum (b), ACF (c) of the NLFM signal with compensation of frequency and phase jumps

Fig. 5 shows the results of modeling only according to (12), since the graph according to (11) is similar to Fig. 2a. In the oscillogram of Fig. 5a, there are no phase distortions at the moments of transitions from one LFM fragment to another, the spectrum of the NLFM signal of Fig. 5b is almost symmetrical, and there are no pulsations on the slopes. The lateral lobes of the ACF of Fig. 5c decay smoothly, the maximum PSLL is  $-22$  dB, and the width of the ML is  $1.8 \mu\text{s}$ .

In comparison with the classical LFM, the PSLL signal decreased by 9 dB, but the price for this is the expansion of the ML of the ACF by almost a third.

## 6 DISCUSSION

Our studies indicate that the use of the new model (12)–(13) provides compensation for jumps in the instantaneous frequency and phase of the NLFM signal at the moments of transition from one LFM fragment to the next, due to which the resulting spectrum becomes symmetrical, rounded, i.e., acquires the expected shape, and there are no pulsations on its slopes.

As a result of the improved spectrum shape, its effective width has increased, and therefore the ML of the ACF has become narrower compared to MM (3)–(4). The lateral lobes of the ACF decrease smoothly, which is also evidence of the absence of frequency-phase distortions.

In the known works [16, 18, 24–25, 28–30], the spectra of the studied NLFM signals are not given, but the given ACFs demonstrate sharp changes in the level and frequency of the lateral lobes, similar to Figures 2d, 3d, 4c, which indicates the presence of instantaneous frequency and phase jumps. In such circumstances, the reduction of the PSLL can be achieved only in some cases by selecting the values of  $T_n$  and  $\Delta f_n$ , which does not ensure the stability and predictability of the final result.

The authors consider it expedient to introduce the three-fragment NLFM signal proposed by the MM into circulation and to continue research in the direction of increasing the number of LFM fragments in order to minimize the PSLL.

## CONCLUSIONS

The scientific novelty of the obtained results is the discovery that frequency and phase jumps during the transition from the first LFM fragment to the second are included as components for determining the magnitude of frequency and phase jumps of the next fragment junction. Based on this, a new MM of the NLFM signal consisting of three LFM fragments is developed. In contrast to the known ones, the proposed model uses the current time instead of the shifted time and compensates for the jumps in the instantaneous frequency and phase of the signal that occur at the moments of transition from one LFM fragment to the next.

The developed model ensures predictability and stability of results when the frequency and time parameters of NLFM signals change.

For the characteristics of the LFM fragments adopted during the modeling, the PSLL of the ACF of the resulting NLFM signal was achieved from  $-22$  dB ( $\Delta f_1 = \Delta f_3 = 125$  kHz,  $\Delta f_2 = 300$  kHz) to  $-27$  dB ( $\Delta f_1 = \Delta f_3 = 55$  kHz,  $\Delta f_2 = 100$  kHz), while the duration of the LFM fragments did not change and was  $T_1 = T_3 = 20$   $\mu$ s,  $T_2 = 100$   $\mu$ s.

The practical significance of obtained results consists in the possibility of using the proposed MM to develop devices for the formation and processing of radio signals in various applications, such as radar systems for detecting air targets, aviation and space systems for surveying the earth's surface, meteorology, sonar, ultrasound diagnostics, etc., in which NLFM signals can be used to reduce the PSLL of the ACF independently or in combination with the WP in the receiving device.

Prospects for further research are to improve the developed model to expand the possibilities of changing the initial frequency and time parameters of the NLFM signals, as well as to study the effect of the number of LFM fragments on the level of the PSLL.

## ACKNOWLEDGEMENTS

We thank the management of Ivan Kozhedub Kharkiv National Air Force University for the opportunity to conduct scientific research.

## REFERENCES

1. Skolnik M. I. Radar Handbook. Editor in Chief. Boston, McGraw-Hill Professional, second edition, 1990, 846 p.
2. Cook C. E., Bernfeld M. Radar Signals: An Introduction to Theory and Application. Boston, Artech House, 1993, 552 p.
3. Barton D. K. Radar System Analysis and Modeling. London, Artech House, 2005, 545 p.
4. Van Trees H. L. Detection, Estimation, and Modulation Theory. New York, John Wiley & Sons, 2004, 716 p.
5. Levanon N., Mozeson E. Radar Signals. New York, John Wiley & Sons, 2004, 403 p.
6. Melvin W. L., Scheer J. A. Principles of modern radar. New York, SciTech Publishing, 2013, 846 p.
7. Doerry A. W. Catalog of Window Taper Functions for Side lobe Control [Electronic resource]. Access mode:

[https://www.researchgate.net/publication/316281181\\_Catalog\\_of\\_Window\\_Taper\\_Functions\\_for\\_Side\\_lobe\\_Control](https://www.researchgate.net/publication/316281181_Catalog_of_Window_Taper_Functions_for_Side_lobe_Control).

8. Heinzel G., Rüdiger A., Schilling R. Spectrum and spectral density estimation by the Discrete Fourier transform (DFT), including a comprehensive list of window functions and some new flattop windows [Electronic resource]. Access mode: [https://pure.mpg.de/rest/items/item\\_52164\\_1/component/file\\_152163/content](https://pure.mpg.de/rest/items/item_52164_1/component/file_152163/content).
9. Galushko V. G. Performance Analysis of using tapered Windows for Side Lobe Reduction in Chirp-Pulse Compression, *Radio Physics and Radio Astronomy*, 2019, Vol. 24(4), pp. 300–313.
10. Nettem A. V., Daniel E. R., Chandu K. Windows For Reduction Of ACF Side Lobes of Pseudo-NLFM Signal, *International Journal of Scientific & Technology Research*, 2019, Vol. 8, Issue 10, pp. 2155–2161.
11. Ghavamirad R., Sebt M. A. Side Lobe Level Reduction in ACF of NLFM Waveform, *IET Radar, Sonar & Navigation*, 2019, Vol. 13, Issue 1, pp. 74–80.
12. Cook C. E. A class of nonlinear FM pulse compression signals, *Proceedings of the IEEE*, 1964, Vol. 52(11), pp. 1369–1371.
13. Cook C. E., Paolillo J. A pulse compression predistortion function for efficient side lobe reduction in a high-power radar, *Proceedings of the IEEE*, 1964, Vol. 52(4), pp. 377–389.
14. Xu Z., Wang X., Wang Y. Nonlinear Frequency-Modulated Waveforms Modeling and Optimization for Radar Applications, *Mathematics*, 2022, Vol. 10, № 3939.
15. Fan Z., Meng H.-Y. Coded excitation with Nonlinear Frequency Modulation Carrier in Ultrasound Imaging System, *IEEE Far East NDT New Technology & Application Forum (FENDT)*. Kunming, Yunnan province, China, 20–22 November 2020, pp. 31–35.
16. Chukka A., Krishna B. Peak Side Lobe Reduction analysis of NLFM and Improved NLFM Radar signal, *AJUB Journal of Science and Engineering (AJSE)*, 2022, Vol. 21, Issue 2, pp. 125–131.
17. Saleh M., Omar S.-M., E. Grivel et al. A Variable Chirp Rate Stepped Frequency Linear Frequency Modulation Waveform Designed to Approximate Wideband Non-Linear Radar Waveforms, *Digital Signal Processing*, 2021, Vol. 109, № 102884.
18. Nettem A. V., Rani E. Doppler Effect Analysis of NLFM Signals, *International Journal of Scientific & Technology Research*, 2019, Vol. 8, Issue 11, pp. 1817–1821.
19. Kurdzo J. M., Cho John Y. N., Cheong B. L. et al. A Neural Network Approach for Waveform Generation and Selection with Multi-Mission Radar, *IEEE Radar Conference*. Boston, 22–26 April 2019, № 19043446.
20. Zhao Y., Ritchie M., Lu X. et al. Non-continuous piecewise nonlinear frequency modulation pulse with variable sub-pulse duration in a MIMO SAR Radar System, *Remote Sensing Letters*, 2020, Vol. 11, Issue 3, pp. 283–292.
21. Xu W., Zhang L., Fang C. et al. Staring Spotlight SAR with Nonlinear Frequency Modulation Signal and Azimuth Non-Uniform Sampling for Low Side Lobe Imaging, *Sensors*, 2021, Vol. 21, Issue 19, № 6487.
22. Song C., Wang Y., Jin G. et al. A Novel Jamming Method against SAR Using Nonlinear Frequency Modulation Waveform with Very High Side Lobes, *Remote Sensing*, 2022, Vol. 14, Issue 21, № 5370.
23. Jin G., Deng Y.-K., Wang R. et al. An Advanced Nonlinear Frequency Modulation Waveform for Radar Imaging With

- Low Side Lobe, *IEEE Transactions on Geoscience and Remote Sensing*, 2019, Vol. 57, Issue 8, pp. 6155–6168.
24. Valli N. A., Rani D. E., Kavitha C. Modified Radar Signal Model using NLFM, *International Journal of Recent Technology and Engineering (IJRTE)*, 2019, Vol. 8, Issue 2S3, pp. 513–516.
25. Adithyavalli N. An Algorithm for Computing Side Lobe Values of a Designed NLFM function, *International Journal of Advanced Trends in Computer Science and Engineering*, 2019, Vol. 8, Issue 4, pp. 1026–1031.
26. Parwana S., Kumar S. Analysis of LFM and NLFM Radar Waveforms and their Performance Analysis, *International Research Journal of Engineering and Technology (IRJET)*, 2015, Vol. 02, Issue 02, pp. 334–339.
27. Bayındır C. A Novel Nonlinear Frequency-Modulated Chirp Signal for Synthetic Aperture Radar and Sonar Imaging, *Journal of Naval Science and Engineering*, 2015, Vol. 11, Issue 1, pp. 68–81.
28. Jeyanthi J. E., Shenbagavalli A., Mani V.R.S. Study of Different Radar Waveform Generation Techniques for Automatic Air Target Recognition, *International Journal of Engineering Technology Science and Research (IJETSRS)*, 2017, Vol. 4, Issue 8, pp. 742–747.
29. Widyantara M. R., Suratman F. Y., Widodo S. et al. Analysis of Non Linear Frequency Modulation (NLFM) Waveforms for Pulse Compression Radar, *Journal Electronica dan Telekomunikasi (JET)*, 2018, Vol. 18, №1, pp. 27–34.
30. Valli N. A., Rani D. E., Kavitha C. Performance Analysis of NLFM Signals with Doppler Effect and Back-ground Noise, *International Journal of Engineering and Advanced Technology (IJEAT)*, 2020, Vol. 9, Issue 3, pp. 737–742.
31. Kostyria O. O., Hryzo A. A., Dodukh O. M. et al. Mathematical model of a two-fragment signal with a non-linear frequency modulation in the current period of time, *Visnyk NTUU KPI Serія – Radiotekhnika Radioaparaturubuduvannia*, 2023, Vol. 92, pp. 60–67.

Received 15.06.2023.

Accepted 26.07.2023.

УДК 621.396.962

## МАТЕМАТИЧНА МОДЕЛЬ ПОТОЧНОГО ЧАСУ ДЛЯ ТРИФРАГМЕНТНОГО РАДІОЛОКАЦІЙНОГО СИГНАЛУ З НЕЛІНІЙНОЮ ЧАСТОТНОЮ МОДУЛЯЦІЄЮ

**Кости́ря О. О.** – д-р техн. наук, старший науковий співробітник, провідний науковий співробітник Харківського національного університету Повітряних Сил імені Івана Кожедуба, Харків, Україна.

**Гризо А. А.** – канд. техн. наук, доцент, начальник НДІ Харківського національного університету Повітряних Сил імені Івана Кожедуба, Харків, Україна.

**Додух О. М.** – канд. техн. наук, провідний науковий співробітник Харківського національного університету Повітряних Сил імені Івана Кожедуба, Харків, Україна.

**Наре́жний О. П.** – канд. техн. наук, доцент кафедри Харківського національного університету імені В. Н. Каразіна, Харків, Україна.

**Федоров А. В.** – д-р філос., науковий співробітник Харківського національного університету Повітряних Сил імені Івана Кожедуба, Харків, Україна.

### АНОТАЦІЯ

**Актуальність.** Одним з напрямків удосконалення існуючих та створення нових радіолокаційних засобів є запровадження зондувальних сигналів з модуляцією частоти (фази), так званих складних сигналів, до яких відносяться сигнали з нелінійною частотною модуляцією. Одним з різновидів цих сигналів є такі, що складаються з трьох лінійно-частотно модульованих фрагментів. Однак широке використання трифрагментних сигналів стримується недостатньою проробкою математичного апарату, який достовірно відображає процеси їх формування та обробки. Авторами статті розроблено нову математичну модель, яка дозволяє враховувати частотні та фазові спотворення, що виникають у трифрагментному сигналі при переході від одного фрагменту до іншого, коли відбувається зміна швидкості частотної модуляції сигналу.

**Мета роботи** – розроблення та дослідження математичної моделі поточного часу для сигналу з нелінійною частотною модуляцією, який складається з трьох лінійно-частотно модульованих фрагментів.

**Метод.** В статті наведено теоретичне обґрунтування необхідності розроблення математичної моделі у поточному часі для трифрагментного сигналу з нелінійною частотною модуляцією, продемонстровано працездатність створеної моделі на прикладі кількох радіосигналів, які відрізняються за частотними параметрами. За однакових сигнальних параметрів здійснено порівняння отриманих результатів з результатами роботи відомої моделі, для чого використовувалися відомі методи спектрального та кореляційного аналізу. Відмінною особливістю запропонованої моделі є врахування стрибків миттєвої частоти і фази сигналу, які виникають під час переходу від одного лінійно-частотно модульованого фрагменту до наступного. Такі стрибкоподібні зміни частоти та фази в відомих моделях сигналів з нелінійною частотною модуляцією не компенсуються, що спричиняє спотворення їх спектрів та збільшення рівня бічних пелюсток авто-кореляційних (взаємно-кореляційних) функцій.

**Результати.** Порівняльна перевірка розробленої та відомої моделей сигналів свідчить про зменшення рівня бічних пелюсток автокореляційної функції на 3 дБ і більше в залежності від заданих частотно-часових параметрів.

**Висновки.** Застосування запропонованої математичної моделі дозволяє формувати та обробляти радіолокаційні сигнали, до складу яких входить три лінійно-частотно модульованих фрагменти. Компенсація стрибкоподібних змін частоти та фази призводить до зменшення ступеня спотворення спектру та, як наслідок, збільшення його ефективної ширини, що забезпечує звуження головної пелюстки та зменшення рівня бічних пелюсток авто-кореляційної функції.

**КЛЮЧОВІ СЛОВА:** радіолокаційний сигнал; нелінійна частотна модуляція; автокореляційна функція, рівень бічних пелюсток; математична модель.

### ЛІТЕРАТУРА

1. Skolnik M. I. Radar Handbook. Editor in Chief / M. I. Skolnik. – Boston : McGraw-Hill Professional, second edition, 1990. – 846 p.
2. Cook C. E. Radar Signals: An Introduction to Theory and Application / C. E. Cook, M. Bernfeld. – Boston : Artech House, 1993. – 552 p.
3. Barton D. K. Radar System Analysis and Modeling / D. K. Barton. – London: Artech House, 2005. – 545 p.
4. Van Trees H. L. Detection, Estimation, and Modulation Theory / H. L. Van Trees. – Edition, reprint : John Wiley & Sons, 2004. – 716 p.
5. Levanon N. Radar Signals / N. Levanon, E. Mozeson. – Hoboken : John Wiley & Sons, 2004. – 403 p.
6. Melvin W. L. Principles of modern radar / W. L. Melvin, J. A. Scheer. – New York : SciTech Publishing, 2013. – 846 p.
7. Doerry A. W. Catalog of Window Taper Functions for Side lobe Control [Electronic resource] / A. W. Doerry. – Access mode: [https://www.researchgate.net/publication/316281181\\_Catalog\\_of\\_Window\\_Taper\\_Functions\\_for\\_Side\\_lobes\\_Control](https://www.researchgate.net/publication/316281181_Catalog_of_Window_Taper_Functions_for_Side_lobes_Control).
8. Heinzel G. Spectrum and spectral density estimation by the Discrete Fourier transform (DFT), including a comprehensive list of window functions and some new flat-top windows [Electronic resource] / G. Heinzel, A. Rüdiger, R. Schilling. – Access mode: [https://pure.mpg.de/rest/items/item\\_152164\\_1/component/file\\_152163/content](https://pure.mpg.de/rest/items/item_152164_1/component/file_152163/content).
9. Galushko V. G. Performance Analysis of using tapered Windows for Side Lobe Reduction in Chirp-Pulse Compression / V. G. Galushko // Radio Physics and Radio Astronomy. – 2019. – Vol. 24(4). – P. 300–313.
10. Nettem A. V. Windows For Reduction Of ACF Side Lobes of Pseudo-NLFM Signal / A. V. Nettem, E. R. Daniel, K. Chandu // International Journal of Scientific & Technology Research. – 2019. – Vol. 8, Issue 10. – P. 2155–2161.
11. Ghavamirad R. Side Lobe Level Reduction in ACF of NLFM Waveform / R. Ghavamirad, M. A. Sebt // IET Radar, Sonar & Navigation. – 2019. – Vol. 13, Issue 1. – P. 74–80.
12. Cook C.E. A class of nonlinear FM pulse compression signals / C. E. Cook // Proceedings of the IEEE. – 1964. – Vol. 52(11). – P. 1369–1371.
13. Cook C. E. A pulse compression predistortion function for efficient side lobe reduction in a high-power radar / C. E. Cook, J. Paolillo // Proceedings of the IEEE. – 1964. – Vol. 52(4). – P. 377–389.
14. Xu Z. Nonlinear Frequency-Modulated Waveforms Modeling and Optimization for Radar Applications / Z. Xu, X. Wang, Y. Wang // Mathematics. – 2022. – Vol. 10, № 3939.
15. Fan Z. Coded excitation with Nonlinear Frequency Modulation Carrier in Ultrasound Imaging System / Z. Fan, H.-Y. Meng // IEEE Far East NDT New Technology & Application Forum (FENDT): Kunming, Yunnan province, China, – 20–22 Nov. 2020. – P. 31–35.
16. Chukka A. Peak Side Lobe Reduction analysis of NLFM and Improved NLFM Radar signal / A. Chukka, B. Krishna // AIUB Journal of Science and Engineering (AJSE). – 2022. – Vol. 21, Issue 2. – P. 125–131.
17. A Variable Chirp Rate Stepped Frequency Linear Frequency Modulation Waveform Designed to Approximate Wideband Non-Linear Radar Waveforms / [M. Saleh, S.-M. Omar, E. Grivel et al.] // Digital Signal Processing. – 2021. – Vol. 109. – № 102884.
18. Nettem A. V. Doppler Effect Analysis of NLFM Signals / A. V. Nettem, E. Rani // International Journal of Scientific & Technology Research. – 2019. – Vol. 8, Issue 11. – P. 1817–1821.
19. A Neural Network Approach for Waveform Generation and Selection with Multi-Mission Radar / [J. M. Kurdzo, Y. N. Cho John, B. L. Cheong et al.] // IEEE Radar Conference: Boston – 22–26 April 2019. – № 19043446.
20. Non-continuous piecewise nonlinear frequency modulation pulse with variable sub-pulse duration in a MIMO SAR Radar System / [Y. Zhao, M. Ritchie, X. Lu et al.] // Remote Sensing Letters. – 2020. – Vol. 11, Issue 3. – P. 283–292.
21. Staring Spotlight SAR with Nonlinear Frequency Modulation Signal and Azimuth Non-Uniform Sampling for Low Side Lobe Imaging / [W. Xu, L. Zhang, C. Fang et al.] // Sensors. – 2021. – Vol. 21, Issue 19. – № 6487.
22. A Novel Jamming Method against SAR Using Nonlinear Frequency Modulation Wave-form with Very High Side Lobes / [C. Song, Y. Wang, G. Jin et al.] // Remote Sensing. – 2022. – Vol. 14, Issue 21. – № 5370.
23. An Advanced Nonlinear Frequency Modulation Waveform for Radar Imaging With Low Side Lobe / [G. Jin, Y.-K. Deng, R. Wang et al.] // IEEE Transactions on Geoscience and Remote Sensing. – 2019. – Vol. 57, Issue 8. – P. 6155–6168.
24. Valli N. A. Modified Radar Signal Model using NLFM / N. A. Valli, D. E Rani, C. Kavitha // International Journal of Recent Technology and Engineering (IJRTE). – 2019. – Vol. 8, Issue 2S3. – P. 513–516.
25. Adithyavalli N. An Algorithm for Computing Side Lobe Values of a Designed NLFM function / N. Adithyavalli // International Journal of Advanced Trends in Computer Science and Engineering. – 2019. – Vol. 8, Issue 4. – P. 1026–1031.
26. Parwana S. Analysis of LFM and NLFM Radar Waveforms and their Performance Analysis / S. Parwana, S. Kumar // International Research Journal of Engineering and Technology (IRJET). – 2015. – Vol. 02, Issue 02. – P. 334–339.
27. Bayındır C. A Novel Nonlinear Frequency-Modulated Chirp Signal for Synthetic Aperture Radar and Sonar Imaging / C. Bayındır // Journal of Naval Science and Engineering. – 2015. – Vol 11, Issue 1. – P. 68–81.
28. Jeyanthi J. E. Study of Different Radar Waveform Generation Techniques for Automatic Air Target Recognition / J. E. Jeyanthi, A. Shenbagavalli, V.R.S. Mani // International Journal of Engineering Technology Science and Research (IJETSr). – 2017. – Vol. 4, Issue 8. – P 742–747.
29. Analysis of Non Linear Frequency Modulation (NLFM) Waveforms for Pulse Compression Radar / [M. R. Widyantara, F. Y. Suratman, S. Widodo et al.] // Journal Electronica dan Telekomunikasi (JET). – 2018. – Vol. 18, №1. – P. 27–34.
30. Valli N. A. Performance Analysis of NLFM Signals with Doppler Effect and Back-ground Noise / N. A. Valli, D. E. Rani, C. Kavitha // International Journal of Engineering and Advanced Technology (IJEAT). – 2020. – Vol. 9, Issue 3. – P. 737–742.
31. Mathematical model of a two-fragment signal with a nonlinear frequency modulation in the current period of time / [O. O. Kostyria, A. A. Hryzo, O. M. Dodukh et al.] // Visnyk NTUU KPI Serii A – Radiotekhnika Radioaparaturbudovannia. – 2023. – Vol. 92. – P. 60–67.